

On the Formation of Aza-ortho-quinone Methides Under Room Temperature Conditions: Cs₂CO₃ Effect

Daniel M. Walden, Ashley A. Jaworski, Ryne C. Johnston, M. Todd Hovey,
Hannah V. Baker, Matthew P. Meyer, Karl A. Scheidt, and Paul Ha-Yeon Cheong

J. Org. Chem., **Just Accepted Manuscript** • DOI: 10.1021/acs.joc.7b00697 • Publication Date (Web): 26 Jun 2017

Downloaded from <http://pubs.acs.org> on June 26, 2017

Just Accepted

“Just Accepted” manuscripts have been peer-reviewed and accepted for publication. They are posted online prior to technical editing, formatting for publication and author proofing. The American Chemical Society provides “Just Accepted” as a free service to the research community to expedite the dissemination of scientific material as soon as possible after acceptance. “Just Accepted” manuscripts appear in full in PDF format accompanied by an HTML abstract. “Just Accepted” manuscripts have been fully peer reviewed, but should not be considered the official version of record. They are accessible to all readers and citable by the Digital Object Identifier (DOI®). “Just Accepted” is an optional service offered to authors. Therefore, the “Just Accepted” Web site may not include all articles that will be published in the journal. After a manuscript is technically edited and formatted, it will be removed from the “Just Accepted” Web site and published as an ASAP article. Note that technical editing may introduce minor changes to the manuscript text and/or graphics which could affect content, and all legal disclaimers and ethical guidelines that apply to the journal pertain. ACS cannot be held responsible for errors or consequences arising from the use of information contained in these “Just Accepted” manuscripts.

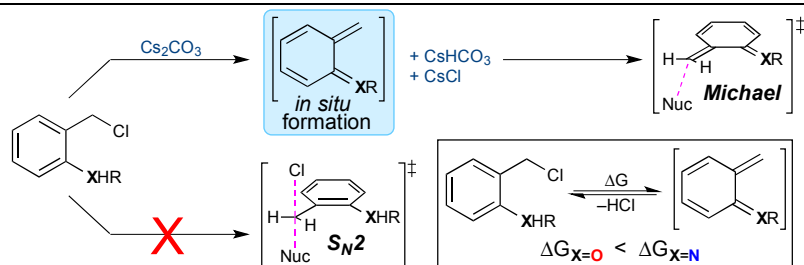
On the Formation of Aza-*ortho*-quinone Methides Under Room Temperature Conditions: Cs₂CO₃ Effect

Daniel M. Walden,[‡] Ashley A. Jaworski,[§] Ryne C. Johnston,[‡] M. Todd Hovey,[§] Hannah V. Baker,[‡] Matthew P. Meyer,[§] Karl A Scheidt^{*,§}, and Paul Ha-Yeon Cheong^{*,‡}

[‡]Department of Chemistry, Oregon State University, 135 Gilbert Hall, Corvallis, OR 97331 (USA)

[§]Department of Chemistry, Northwestern University 2145 Sheridan Rd, Evanston, IL 60208 (USA)

[§]Department of Chemistry and Biochemistry, University of California, Merced, CA 95453 (USA)

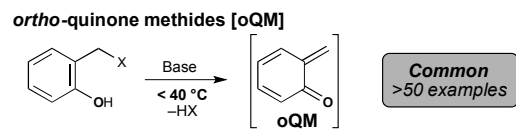


ABSTRACT: Since the first report of a facile, room temperature process to access aza-ortho-quinone methides (aoQMs) by Corey in 1999, this chemistry has remained dormant until our report of an enantioselective catalytic example in 2014. We report a theoretical & experimental study of the key to success behind these successful examples to enable broader exploitation of this useful intermediate. We have discovered that transformations involving the aoQM are remarkably facile with barriers <17 kcal/mol. The main difficulty of exploiting aoQM in synthesis is that they are unstable ($\Delta G = \sim 30$ kcal/mol), precluding their formation under mild conditions. The use of Cs₂CO₃ as base is critical. It provides a thermodynamically and kinetically favorable means to form aoQMs, independent of the salt solubility and base strength. The exothermic formation of salt byproducts provides a driving force (average $\Delta G = -31.1$ kcal/mol) compensating for the majority of the inherent unfavorable thermodynamics of aoQM formation.

INTRODUCTION

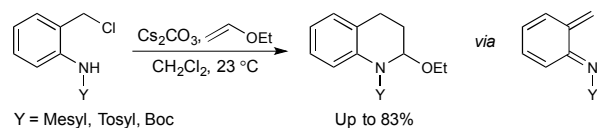
Quinone methides, particularly *ortho*-quinone methides (oQMs), are highly reactive and useful intermediates¹ with numerous examples in synthetic methodologies,² total syntheses,³ and natural product chemistry.⁴ A multitude of reports disclose oQM use under mild conditions.⁵ In contrast, reports of *in situ* generation of aza-ortho-quinone methides (aoQMs) as reactive intermediates under mild conditions are demonstrably rare (Scheme 1, Top).⁶ E. J. Corey first reported the use of aoQMs as useful reactive intermediates in 1999,⁷ and for more than a decade, this chemistry remained underexplored until our report in 2014.⁸ While there are examples of aoQMs being formed as a result of pyrolysis, photolysis, with non-removable stabilizing groups⁹ or from even more reactive precursors,¹⁰ the difficulty of its generation under mild conditions have limited aoQMs as general electrophiles in catalysis and synthesis.

In this report, we studied three reactions that can proceed through aoQM intermediacy using experiments and theory.¹¹ We have identified the enabling factor behind successful cases of aoQM-mediated reactions under mild conditions. Herein, we describe the thermodynamic and kinetic effect Cs₂CO₃ has in accessing the reactive aoQM intermediate in synthesis and asymmetric catalysis. Our results highlight and refine the cesium effect¹² that has been at the forefront of many organic reactions that take place under basic conditions. While this current study focuses on the use of *ortho* substituted benzyl chloride precursors as substrates, we will continue to leverage our newfound understanding to develop novel substrates for aoQM-mediated reactions.

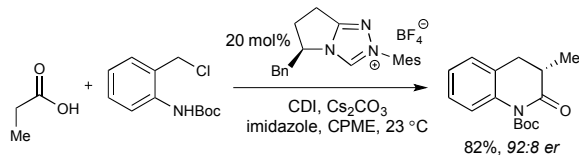


- more controlled conditions
- opportunities for asymmetric catalysis

Corey, *Angewandte Chemie* 1999



Our work, *J. Am. Chem. Soc.* 2014



Scheme 1. Summary of oQM chemistry and recent aoQM chemistry.

RESULTS AND DISCUSSION

Computational details. Geometry optimizations were performed with the Mo6-2X method¹³ with SDD+ECP for Cs and 6-31G(d)¹⁴ basis sets for all other atoms. Solvation was modelled implicitly¹⁵ using PCM¹⁶ with the solvent employed in the experiments. Geometry optimizations, vibrational frequency analysis, and PCM solvation was completed using Gaussian 09.¹⁷ Energy refinements were computed at Mo6-2X/def2-QZVPP¹⁸ using the ORCA computational package¹⁹ with PCM solvation corrections at Mo6-2X/6-311++G(2df,p)²⁰ & SDD+ECP using Gaussian 09.

Reliable energetics involving partially heterogeneous, strongly ionic acid/base reactions in which constituent reactants, intermediates, or products can potentially dimerize/oligomerize are theoretically challenging at present, and these results should be taken as a model process that assumes homogeneity, precluding nucleation/oligomerization and other experimental anomalies. Regardless, the key discovery here is that the Cs₂CO₃ is critical in effecting aoQM formation under mild conditions.

Inherent stability of aoQM vs. oQM. The discrepancy between the proliferation of oQM over aoQM mediated reactions was first investigated. We evaluated the effect of the heteroatom on the quinone equilibria. The computed equilibria in dichloromethane, diethylether, and tetrahydrofuran between the *ortho* substituted benzyl chloride precursor and their corresponding methides are shown in Table 1. The oQM is more stable than the aoQM by ~10 kcal/mol, corresponding to ~10⁷-fold ease of forming the oQM at room temperature. This may explain the

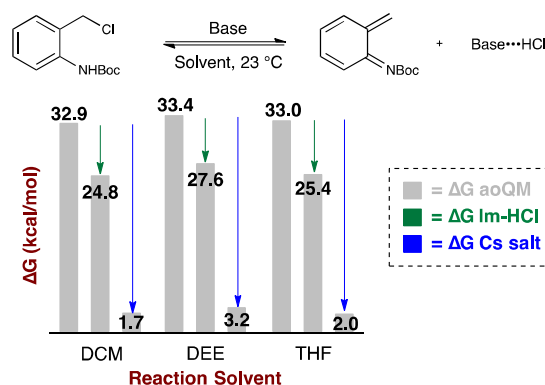
prevalence of the former in literature. The stability differences are attributed to the relative π -bond strengths between carbon and the heteroatoms. The stronger, more polarized C=O π -bond in the oQM derivatives helps mitigate the energetic penalty of losing aromaticity. The C=O π -bond is stronger than C=N π -bond by 10–15 kcal/mol, matching the stability differences between oQM and aoQM.²¹

Table 1. Computed *ortho*-quinone and *aza-ortho*-quinone methide equilibria.

X	ΔG (DCM)	ΔG (DEE)	ΔG (THF)
O	19.6	19.9	19.7
NH	29.1	29.3	29.1
NBoc	32.9	33.4	33.0

Cesium carbonate equilibrium facilitates aoQM production. Any reaction which generates methides must overcome the resonance energy of benzene.²² Under harsh conditions, much of this energy will come from light or heat. Under milder reaction conditions, the harnessing of chemical energy will play a much larger role. We postulated that the basic conditions used to generate these reactive intermediates may be responsible in mitigating the unfavorable thermodynamics. Specifically, we considered the thermodynamic effect of converting Cs₂CO₃ and HCl to CsHCO₃ and CsCl. Computations showed that this reaction is highly exergonic in three different polar aprotic solvents ($\Delta G_{\text{avg}} = -30.8$ kcal/mol, blue arrows, Chart 1). By coupling this reaction with the aoQM formation process, aoQMs were now shown to be in equilibrium with the *ortho* amino benzyl chloride precursors under ambient conditions (ΔG aoQM 1.7–3.2 kcal/mol).

Chart 1. The affect of in situ salt formation on aoQM thermodynamics with imidazole and cesium carbonate as base.



We wondered if other more moderate bases such as imidazole behave similarly. Computations suggested that the complexation of an imidazole to the *in situ* generated HCl puts the NBoc-protected aoQM at ~ 25 kcal/mol ($\Delta G_{\text{avg}} = 25.9$ kcal/mol, Chart 1, green arrows). The thermodynamic stabilization afforded by the formation of an imidazole-HCl complex is ~ 8 kcal/mol, which would predict little aoQM formation at room temperature from thermodynamics alone.²³

Mechanistic analysis of aoQM formation. Three pathways for aoQM formation can be envisioned (Figure 1), beginning with fast deprotonation of the labile amine proton by cesium carbonate (**TS-Deprotonation**, $\Delta G^\ddagger = 3.6$ kcal/mol). All computed mechanisms originate from the post-deprotonation cesium complex ($\Delta G = 0.4$ kcal/mol). Two modes of intramolecular S_N2 attack²⁴ followed by electrocyclic ring opening were considered (magenta and blue pathways). While the barrier of **6-exo-tet-TS** ($\Delta G^\ddagger = 24.6$ kcal/mol) lies close to the estimated experimental barrier, the intermediate that follows presents a significant thermodynamic sink ($\Delta G = -18.1$ kcal/mol). The stability of this intermediate hinders **Oxazine-opening-TS** from occurring, even if electrocyclic ring opening gives a reasonable barrier from starting material ($\Delta G^\ddagger = 21.4$ kcal/mol). The computed barrier to **Oxazine-opening-TS** of 39.5 kcal/mol (relative to the benzoxazine intermediate) is consistent with computed and experimental barriers of retro-Diels-Alder reactions of 1,2-benzoxazines to form oQMs.²⁵ A similar trend is observed for **6-exo-tet-TS**, although both the initial ring closure ($\Delta G^\ddagger = 33.7$ kcal/mol) and **Azididine-opening-TS** ($\Delta G^\ddagger = 38.8$ kcal/mol) are highly disfavored regardless of the thermodynamics of the fused ring intermediate. Ultimately, simple elimination of the chloride leaving group is computed as the favored pathway (**Elimination-TS**, $\Delta G^\ddagger = 12.1$ kcal/mol).

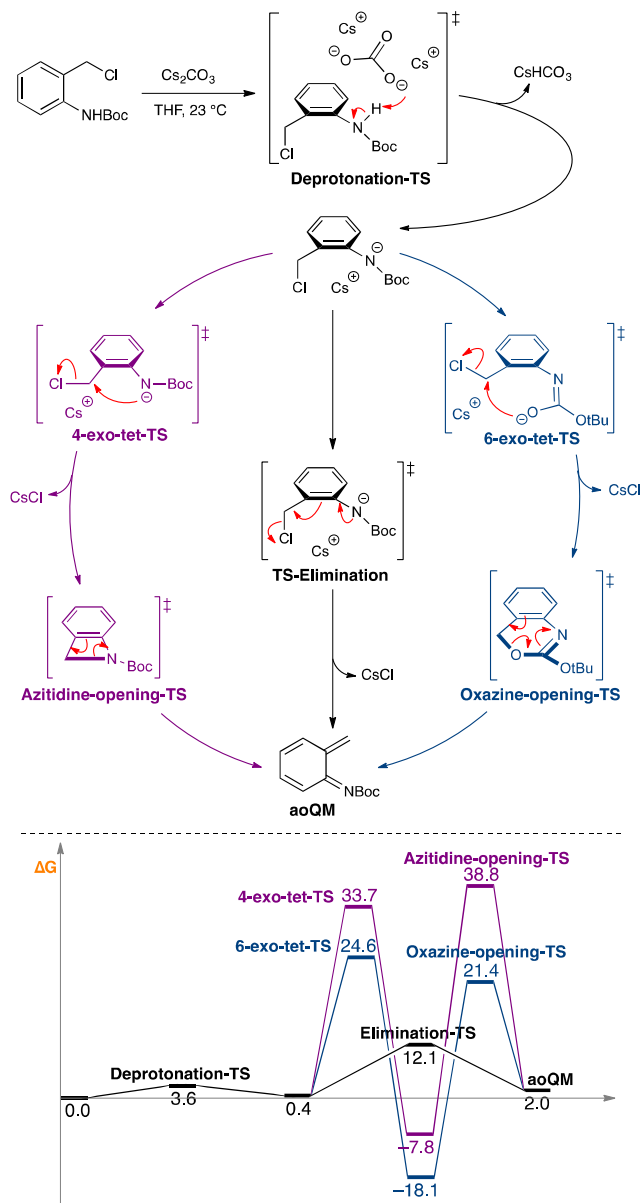


Figure 1. Computed mechanisms of aoQM formation in THF solvent. Stepwise deprotonation followed by chloride elimination is the favored mechanism (black) over intramolecular S_N2 and ring-opening (blue and magenta).

Elimination of the chloride leaving group results in loss of aromaticity, typically seen as a formidable hurdle in most room temperature reactions. Complexation of the cesium cation with the departing leaving group and the partially anionic nitrogen atom (Figure 2, **Elimination-TS**) is hypothesized to offset this penalty to the point of facile aoQM formation under ambient conditions. Considering that the equilibrium between the *ortho* substituted benzyl chloride precursor and cesium bicarbonate slightly favors the starting material by 0.4 kcal/mol, it is proposed that the main driving force is the formation of the ionic Cs-Cl bond itself. This effect is apparent in the highly exergonic formation of the fused azitidine ($\Delta G = -7.8$ kcal/mol) and oxazine ring ($\Delta G = -18.1$ kcal/mol) intermediates (Figure 1, Bottom), where aromaticity is in-

tact and ring formation is concomitant with CsCl salt formation.

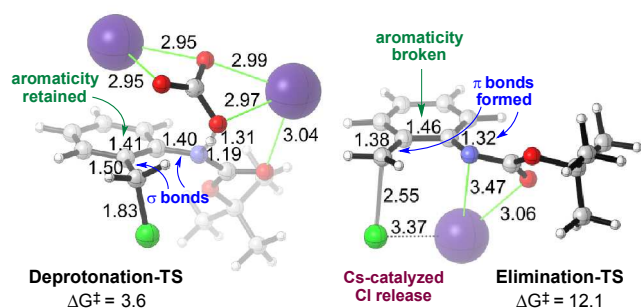
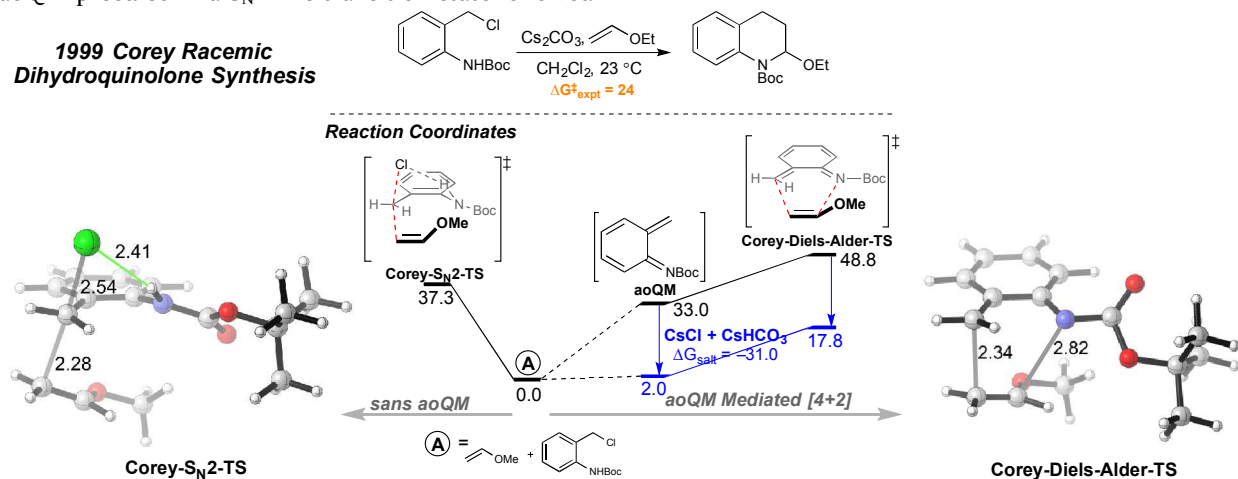


Figure 2. Computed TSs²⁶ of the stepwise deprotonation/elimination mechanism for aoQM formation.

Applications to dihydroquinolone synthesis. Corey's dihydroquinolone reaction was hypothesized to occur via a concerted or stepwise Diels-Alder to an aoQM generated *in situ*. From our previous computations, we can already predict that the cesium carbonate in solution will render the aoQM accessible under room temperature conditions. What is unknown is whether an alternative mechanism competes with the subsequent cycloaddition step. One such possible mechanism is direct nucleophilic substitution, in which the vinyl ether may directly add to the aoQM precursor via S_N2-like transition state followed

by loss of HCl and cyclization to furnish the observed dihydroquinolone product (**Corey-S_N2-TS**, Figure 3, Top panel). The developing negative charge of the departing chloride is stabilized by the vicinal N-H (2.41 Å). Even with the anionic Cl leaving group stabilized through hydrogen bonding, the S_N2 barrier is considerably high (37.3 kcal/mol). The most favorable pathway is formation of the aoQM (ΔG = 2.0 kcal/mol) followed by concerted [4+2] (**Corey-Diels-Alder-TS**, ΔG[‡] = 17.8 kcal/mol). In the absence of cesium carbonate, no reaction is expected to occur given the high energy of the S_N2 (ΔG[‡] = 37.3 kcal/mol) and [4+2] (ΔG[‡] = 48.8 kcal/mol) pathways, both which lie far below the estimated barrier of 24 kcal/mol.

Analysis of the NHC-catalyzed asymmetric dihydroquinolone synthesis reveals similar energetic trends (Figure 3, Bottom panel). While the nucleophilic substitution pathway is lower in energy than the Corey example (S_N2-TS, ΔG[‡] = 29.2 kcal/mol), it still lies above the estimated room temperature barrier, and significantly below the **Major-Michael-TS** (ΔG[‡] = 13.5 kcal/mol) as mediated by aoQM formation. Dihydroquinolone formation is stepwise, beginning with Michael addition and followed by cyclization (**Cyclization-TS**, ΔG[‡] = -15.2 kcal/mol). Release of the NHC from the resultant tetrahedral intermediate leads to product and begins a new catalytic cycle.



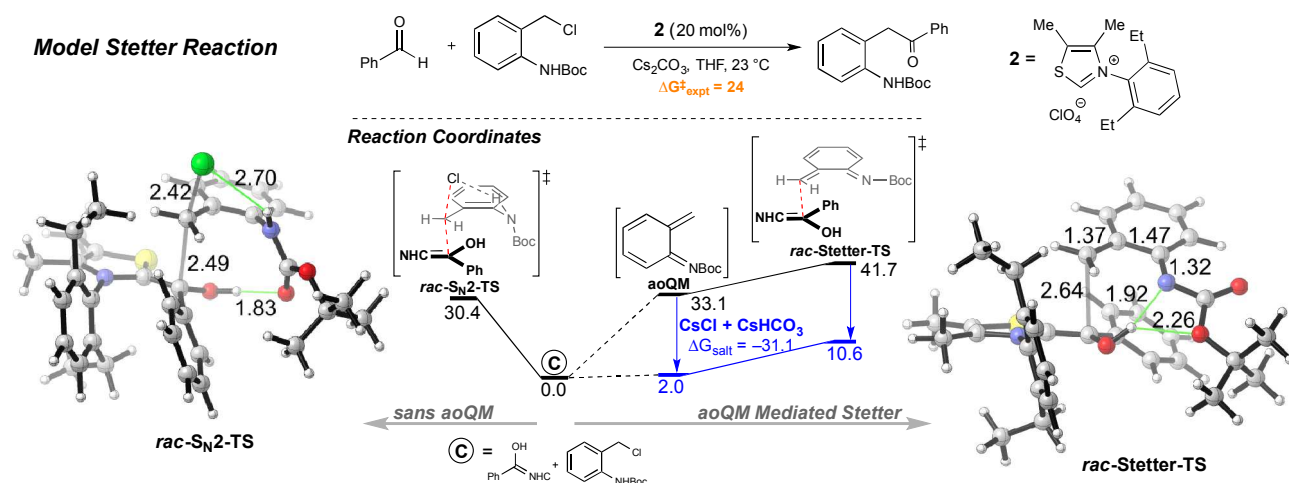
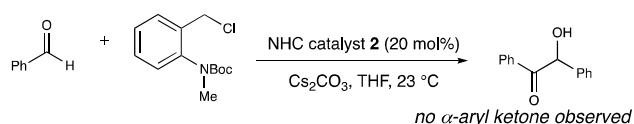


Figure 5. NHC **2**-catalyzed Stetter-type reaction of benzaldehyde. Bidirectional reaction coordinate diagrams shown. To the right, two energetics for the aoQM-mediated reaction: parent reaction without formation of any salt byproducts (black) and with Cs_2CO_3 salt byproducts ($\text{CsCl} + \text{CsHCO}_3$, blue). To the left, energetics for the non-aoQM mediated $\text{S}_{\text{N}}2$ process.

In comparing the experimental and computed^{30,31} isotope effects, *rac-S_N2-TS* and *rac-Stetter-TS* both showed significant KIE deviations only at C₁, but the latter was in better agreement with experiments (7.3% vs. 2.7% error at C₁, Figure 6). Computed equilibrium isotope effects for the formation of the aoQM intermediate were more consistent with experimental values, and suggested this step may be rate determining. While equilibrium isotope effects are not rigorous substitutes for comparison with experimental KIE measurements, they offer a valid approximation, considering that the transition state immediately prior to aoQM formation is product-like in geometry.



Furthermore, the *N*-methylated precursor, which cannot form the aoQM, did not provide any α -aryl ketone product after 48 hours, instead yielding exclusively the benzoin adduct (Scheme 2). This suggested that the preclusion of the aoQM dramatically slowed down the Stetter process. We anticipated that methylation of the substrate might also affect the barrier of the nucleophilic addition step. The computed barrier of 30.3 kcal/mol (Figure 7, *Me-rac-S_N2-TS*) is essentially identical to *rac-S_N2-TS* ($\Delta G^\ddagger = 30.4$ kcal/mol), indicating that methylation likely shuts down aoQM formation/deprotonation step without targeting the $\text{S}_{\text{N}}2$ pathway.

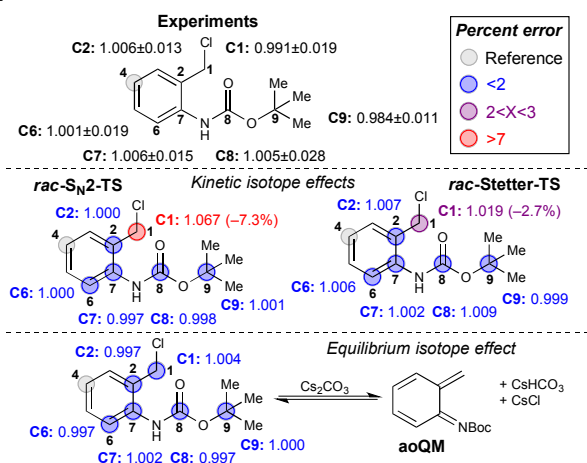


Figure 6. Natural abundance isotope effects (IE) results. Experiments (Top, average of triplicate runs \pm standard deviations), computed kinetic IE for $\text{S}_{\text{N}}2$ and Stetter (Middle) and equilibrium IE (Bottom).

Scheme 2. Effect of Substrate *N*-Methylation on the NHC-Catalyzed Stetter Reaction.

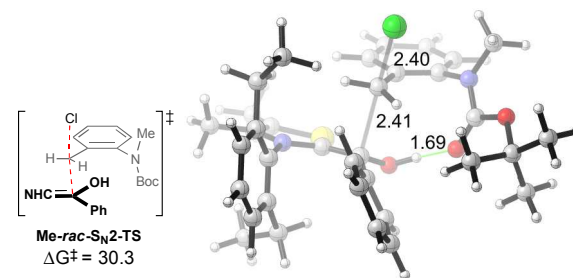
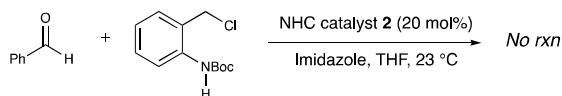


Figure 7. Computed methylated Stetter $\text{S}_{\text{N}}2$ TS showing a similar barrier to the non-methylated parent *rac-S_N2-TS*.

Analysis of the formation of imidazole-HCl indicated that while exergonic, the ~ 8 kcal/mol stabilization provided was not enough to drive aoQM formation (Chart 1). As an experimental test, the model Stetter reaction (Figure 5) was run with imidazole as base in place of Cs_2CO_3 . As predicted by theory, there was no reaction with imid-

azole base (Scheme 3). These computations and experiments, in combination with the isotope effect data, provided evidence supporting aoQM intermediacy for low temperature aoQM mediated processes (Figures 3 and 4).

Scheme 3. Effect of Imidazole Base on the NHC-Catalyzed Stetter Reaction.



CONCLUSIONS

To summarize, we have combined theory and experiments towards the understanding of the synthetic accessibility of aza-ortho-quinone methides, an underutilized reactive synthetic intermediate with significant potential. Specifically, we have discovered what enables the formation of aoQM as viable reaction intermediates in synthesis under room temperature conditions. The loss of aromaticity over the course of the methide formation is balanced by the exergonic formation of metal chloride and metal bicarbonate salts (>30 kcal/mol), an independent effect from salt solubility and strength of the base. This energetic trade off is distinctly different from the parent oQMs, where the relative strength of the C=O π bond is enough to render this species accessible even in the absence of this thermodynamic and kinetic Cs_2CO_3 effect. The impact of salt formation in organocatalysis, especially in rendering high energy reactive intermediates thermodynamically accessible, is currently not well understood. We illustrate a thorough and enabling understanding that allows the community to leverage the utility and unique reactivity of aoQMs in asymmetric catalysis and chemical synthesis. These discoveries will enable a broader discovery and development platform integrating mild aoQM generation and its use in catalytic reactions, as oQM has for decades.

EXPERIMENTAL

KIE Experimental Parameters: Data was collected from a total of three Stetter reactions taken to 90.0%, 88.8% and 89.7% completion respectively.³² The unreacted benzyl chloride from the model Stetter reaction with catalyst 2 and benzaldehyde was recovered and analyzed by quantitative ^{13}C NMR spectroscopy (see supporting information). All samples were prepared identically as described: 60 mg of recovered starting material was dissolved in 0.5 mL of CDCl_3 and then filtered through a 3 mm plug of celite directly into a 5 mm high-precision NMR tube. Each NMR tube was filled to a constant sample height of 5 cm. Spectra were acquired on a Bruker Avance III 500 MHz spectrometer using proton-decoupled pulses with 80 s delays between pulses. 65536 data points were collected, which were then zero-filled to 256k before Fourier transformation. A zeroth order baseline correction was applied to all spectra, and integrations were measured using a ± 0.5 ppm region centered on each peak. The starting benzyl chloride used in all reactions and reference measurements came from the same synthetic batch. T_1 values were measured for each sample using the inversion-recovery method to ensure the absence of any paramagnetic impurities.

General Procedure for NHC-catalyzed addition of benzaldehyde to aza-oQMs: *tert*-Butyl (2-(chloromethyl)phenyl)carbamate (1.209 g, 5 mmol), 3-(2,6-diethylphenyl)-4,5-dimethylthiazol-3-ium perchlorate 2 (0.346 g, 1.00 mmol), 2-methoxynaphthalene (NMR internal standard, 0.395 g, 2.500 mmol), and freshly dried and powdered cesium carbonate (1.955 g, 6.00 mmol) were combined in an oven-dried 250 mL round bottom flask fitted with a magnetic stirbar under argon. The reaction flask was evacuated under reduced pressure for 15 minutes, then back-filled with argon 3 times. THF (50 mL) was added and the mixture was stirred for 30s, until all soluble materials went into solution. A 100 μL aliquot was taken for NMR analysis (T_0). Benzaldehyde (0.612 mL, 6.00 mmol) was added to the flask via syringe, and the reaction vessel was sealed and stirred vigorously under static argon. 100 μL aliquots were taken periodically to monitor consumption of the starting material. When an NMR aliquot indicated high (~90%) conversion (12–16h), the entire reaction mixture was filtered through a 1 cm pad of Celite and a final aliquot of the filtrate was taken to determine the percent conversion of benzyl chloride at the end timepoint (T_i). The filtered reaction mixture was concentrated under reduced pressure, and the residue was applied to a 2-inch pad of silica gel. Elution with 4:1 hexanes:ethyl acetate (until all remaining starting material had been collected, ~200 mL, TLC monitoring) followed by concentration of the eluent provided the crude recovered starting material. The recovered benzyl chloride was further purified by elution on a 50 g SNAP biotage column, (gradient 2–15% hexanes:ethyl acetate, 14 column volumes). The pure fractions of recovered benzyl chloride were collected, concentrated, dried under reduced pressure and then analyzed by quantitative ^{13}C NMR spectroscopy (see supporting information for details).

ASSOCIATED CONTENT

Supporting Information

Cartesian coordinates, energies, experimental and computational KIE data, additional figures, and characterization of new compounds. The Supporting Information is available free of charge on the ACS Publications website.

AUTHOR INFORMATION

Corresponding Author

paulc@science.oregonstate.edu;

scheidt@northwestern.edu

ACKNOWLEDGMENT

PHYC is the Bert and Emelyn Christensen professor of OSU, and gratefully acknowledges financial support from the Stone family and the National Science Foundation (NSF, CHE-1352663). We thank Dr. Yuyang Wu (NU) for assistance with KIE experiments. KAS gratefully acknowledges support from the National Institutes of Health (NIGMS R01 GM073072). DMW, RCJ, and PHYC also acknowledge computing infrastructure in part provided by the NSF Phase-2 CCI, Center for Sustainable Materials Chemistry (NSF CHE-1102637). DMW also acknowledges support from the Johnson Research Fellowship.

REFERENCES

¹ Jaworski, A. A.; Scheidt, K. A. *J. Org. Chem.* **2017**, *81*, 10145–10153.

² For examples of oQMs in methodology, see: (a) Song, L.; Yao, H.; Tong, R.; *Org. Lett.* **2014**, *16*, 3740–3743. (b) Spence, J. T. J.; George, J. H.; *Org. Lett.* **2013**, *15*, 3891–3893. (c) Liao, D.; Li, H.; Lei, X. *Org. Lett.* **2012**, *14*, 18–21. (d) Angle, S. R.; Yang, W. *J. Am. Chem. Soc.* **1990**, *112*, 4524–4528. (e) Ito, Y.; Nakajo, E.; Nakatsuka, M.; Saegusa, T. *Tet. Lett.* **1983**, *24*, 2881–2884.

³ For examples of oQMs in total synthesis, see: (a) Jeffrey, C. S.; Leonard, M. D.; Glassmire, A. E.; Dodson, C. D.; Richards, L. A.; Kato, M. J.; Dyer, L. A. *J. Nat. Prod.* **2014**, *77*, 148–153. (b) Li, H.; Jiang, J.; Liu, Z.; Lin, S.; Xia, G.; Xia, X.; Ding, B.; He, L.; Lu, Y.; She, Z. *J. Nat. Prod.* **2014**, *77*, 800–806.

⁴ For examples of oQMs in natural product chemistry, see: (a) Gnaim, S.; Shabat, D. *Acc. Chem. Res.* **2014**, *47*, 2970–2984. (b) El-Sepelgy, O.; Haseloff, S.; Alamsetti, S. K.; Schneider, C. *Angew. Chem. Int. Ed.* **2014**, *53*, 7923–7927. (c) Verga, D.; Nadai, M.; Doria, F.; Percivalle, C.; Antonio, M. D.; Palumbo, M.; Richter, S. N.; Freccero, M. *J. Am. Chem. Soc.* **2010**, *132*, 14625–14637. (d) Doria, F.; Richter, S. N.; Nadai, M.; Colloredo-Mels, S.; Mella, M.; Palumbo, M.; Freccero, M. *J. Med. Chem.* **2007**, *50*, 6570–6579.

⁵ For examples of low temperature oQM formation, see: (a) Lewis, R. S.; Garza, C. J.; Dang, A. T.; Pedro, T. K. A.; Chain, W. J. *Org. Lett.* **2015**, *17*, 2278–2281. (b) Bai, W.-J.; David, J. G.; Feng Z.-G.; Weaver, M. G.; Wu, K.-L.; Pettus, T. R. *Acc. Chem. Res.* **2014**, *47*, 3655–3664 and references cited therein. (c) Izquierdo, J.; Orue, A.; Scheidt, K. A. *J. Am. Chem. Soc.* **2013**, *135*, 10634–10637.

⁶ For an example of slow aoQM formation even with heat, acid, base, and electrophilic activation, see: Frank, K. E.; Aubé, J. *J. Org. Chem.* **2000**, *65*, 655–666.

⁷ (a) Steinhagen, H.; Corey, E. J. *Angew. Chem. Int. Ed.* **1999**, *38*, 1928–1931. (b) Steinhagen, H.; Corey, E. J. *Org. Lett.* **1999**, *1*, 823–824.

⁸ Lee, A.; Younai, A.; Price, C. K.; Izquierdo, J.; Mishra, R. K.; Scheidt, K. A. *J. Am. Chem. Soc.* **2014**, *136*, 10589–10592.

⁹ Liao, H.-H.; Chatupheeraphat, A.; Hsiao, C.-C.; Atodiressei, I.; Rueping, M. *Angew. Chem. Int. Ed.* **2015**, *54*, 15540–15544.

¹⁰ For a review of aoQMs in organic synthesis, see: Wojciechowski, K. *Eur. J. Org. Chem.* **2001**, *19*, 3587–3605.

¹¹ This approach may avoid potential pitfalls of relying on only theory or only experiments: (a) Clemente, F. R.; Houk, K. N. *Angew. Chem. Int. Ed.* **2004**, *43*, 5766–5768. (b) Plata, R. E.; Singleton, D. A. *J. Am. Chem. Soc.* **2015**, *137*, 3811–3826. (c) Zhu, H.; Clemente, F. R.; Houk, K. N.; Meyer, M. P. *J. Am. Chem. Soc.* **2009**, *131*, 1632–1633.

¹² The cesium effect is the ability of cesium bases to promote higher reactions yields over other bases, including their sodium and potassium analogs. See: (a) Martinez-Ariza, G.; McConnell, N.; Hulme, C. *Org. Lett.* **2016**, *18*, 1864–1867. (b) Xu, H.; Muto, K.; Yamaguchi, J.; Zhao, C.; Itami, K.; Musaev, D. G. *J. Am. Chem. Soc.* **2014**, *136*, 14834–14844. (c) Salvatore, R. N.; Nagle, A. S.; Jung, K. W. *J. Org. Chem.* **2002**, *67*, 674–683. (d) Haféz, A. M.; Taggi, A. E.; Wack, H.; Esterbrook, J.; Lectka, T. *Org. Lett.* **2001**, *3*, 2049–2051. (e) *J. Prakt. Chem.* **1999**, *341*, 186–190. (f) Kunz, H.; Kullmann, R.; Wernig, P.; Zimmer, J. *Tetrahedron Lett.* **1992**, *33*, 1969–1972. (g) Dijkstra, G.; Kruizinga, W. H.; Kellogg, R. M. *J. Org. Chem.* **1987**, *52*, 4230–4234.

¹³ Zhao, Y.; Truhlar, D. G. *Theor. Chem. Acc.* **2008**, *120*, 215–241.

¹⁴ Hehre, W. J.; Ditchfield, R.; Pople, J. A. *J. Chem. Phys.* **1972**, *56*, 2257–2261.

¹⁵ The equilibrium of cesium carbonate and HCl with cesium bicarbonate and cesium chloride was investigated with explicit THF solvation in the geometry optimizations (See Supporting Information, Figure S1). The equilibrium remains highly exergonic ($\Delta G = -43$ kcal/mol), and in line with the conclusions granted from Chart 1.

¹⁶ S. Miertuš, S.; Scrocco, E.; Tomsai, J. *Chem. Phys.* **1981**, *55*, 117–129.

¹⁷ Gaussian 09, Revision D.01, Frisch, M. J.; Trucks, G. W.; Schlegel, H. B.; Scuseria, G. E.; Robb, M. A.; Cheeseman, J. R.; Scalmani, G.; Barone, V.; Mennucci, B.; Petersson, G. A.; Nakatsujii, H.; Caricato, M.; Li, X.; Hratchian, H. P.; Izmaylov, A. F.; Bloino, J.; Zheng, G.; Sonnenberg, J. L.; Hada, M.; Ehara, M.; Toyota, K.; Fukuda, R.; Hasegawa, J.; Ishida, M.; Nakajima, T.; Honda, Y.; Kitao, O.; Nakai, H.; Vreven, T.; Montgomery, J. A., Jr.; Peralta, J. E.; Ogliaro, F.; Bearpark, M.; Heyd, J. J.; Brothers, E.; Kudin, K. N.; Staroverov, V. N.; Kobayashi, R.; Normand, J.; Raghavachari, K.; Rendell, A.; Burant, J. C.; Iyengar, S. S.; Tomasi, J.; Cossi, M.; Rega, N.; Millam, J. M.; Klene, M.; Knox, J. E.; Cross, J. B.; Bakken, V.; Adamo, C.; Jaramillo, J.; Gomperts, R.; Stratmann, R. E.; Yazyev, O.; Austin, A. J.; Cammi, R.; Pomelli, C.; Ochterski, J. W.; Martin, R. L.; Morokuma, K.; Zakrzewski, V. G.; Voth, G. A.; Salvador, P.; Dannenberg, J. J.; Dapprich, S.; Daniels, A. D.; Farkas, Ö.; Foresman, J. B.; Ortiz, J. V.; Cioslowski, J.; Fox, D. J. Gaussian, Inc., Wallingford CT, 2009.

¹⁸ Wiegand, F.; Ahlrichs, R. *Phys. Chem. Chem.* **2005**, *7*, 3297–3305.

¹⁹ Neese, F. *WIREs Comput. Mol. Sci.* **2012**, *2*, 73–78.

²⁰ Hariharan, P. C.; Pople, J. A. *Theor. Chim. Acta* **1973**, *28*, 213–222.

²¹ Kerr, J. A. *Chem. Rev.* **1966**, *66*, 465–500.

²² (a) Pauling, L.; Wheland, G. W. *J. Chem. Phys.* **1933**, *1*, 362–374. (b) Hess, Jr. B. A.; Schaad, L. J. *J. Am. Chem. Soc.* **1983**, *105*, 7500–7505.

²³ Estimated room temperature (23 °C) barriers were calculated based on reaction yield and time using the Eyring equation: Eyring, H. *J. Chem. Phys.* **1935**, *3*, 107–115.

²⁴ Baldwin, J. E. *J. Chem. Soc., Chem. Commun.* **1976**, *18*, 734–736.

²⁵ Sugimoto, H.; Nakamura, S.; Ohwada, T. *J. Org. Chem.* **2007**, *72*, 10088–10095.

²⁶ Structure images generated using the CylView molecular visualization program: C. Y. Legault *CYLview*, version 1.0b; Université Sherbrooke: Quebec, Canada, 2009; <http://www.cylview.org>.

²⁷ Walden, D. M.; Ogba, O. M.; Johnston, R. C.; Cheong, P. H.-Y. *Acc. Chem. Res.* **2016**, *49*, 1279–1291.

²⁸ Johnston, R. C.; Cheong, P. H.-Y. *Org. Biomol. Chem.* **2013**, *11*, 5057–5064.

²⁹ Singleton, D. A.; Thomas, A. A. *J. Am. Chem. Soc.* **1995**, *117*, 9357–9358.

³⁰ Isotope effects calculated using the Onyx program: Brueckner, A. C.; Cevallos, S. L.; Ogba, O. M.; Walden, D. M.; Meyer, M. P.; O’Leary, D. J.; Cheong, P. H.-Y. *Onyx*, version 1.0; Oregon State University: Corvallis, OR, USA, 2016.

³¹ (a) Bigeleisen, J.; Mayer, M. G. *J. Chem. Phys.* **1947**, *15*, 261–267. (b) Bell, R. P. *The Tunnel Effect in Chemistry*. New York: Chapman and Hall; 1980. (c) Northrop, D. B. *J. Am. Chem. Soc.* **1999**, *121*, 3521–3524.

³² Conversions were calculated relative to an internal standard using ¹H NMR spectroscopy.

1
2
3
4
5
6
7
8
9
10
11
12
13
14
15
16
17
18
19
20
21
22
23
24
25
26
27
28
29
30
31
32
33
34
35
36
37
38
39
40
41
42
43
44
45
46
47
48
49
50
51
52
53
54
55
56
57
58
59
60